ACADEMIC PRESS

Available online at www.sciencedirect.com

SCIENCE DIRECT®

DEVELOPMENTAL BIOLOGY

Developmental Biology 253 (2003) 200–213

www.elsevier.com/locate/ydbio

Autonomous and nonautonomous functions for Hox/Pbx in branchiomotor neuron development

Kimberly L. Cooper,[a] Wendy M. Leisenring,[b] and Cecilia B. Moens[a,*]

[a] *Howard Hughes Medical Institute, Division of Basic Science, Fred Hutchinson Cancer Research Center, 1100 Fairview Ave. N., Seattle, WA 98109, USA*

[b] *Clinical Statistics, Clinical Research Division, Fred Hutchinson Cancer Research Center, 1100 Fairview Ave. N., Seattle, WA 98109, USA*

Received for publication 26 August 2002, revised 4 October 2002, accepted 9 October 2002

Abstract

The vertebrate branchiomotor neurons are organized in a pattern that corresponds with the segments, or rhombomeres, of the developing hindbrain and have identities and behaviors associated with their position along the anterior/posterior axis. These neurons undergo characteristic migrations in the hindbrain and project from stereotyped exit points. We show that *lazarus/pbx4*, which encodes an essential *Hox* DNA-binding partner in zebrafish, is required for facial (VIIth cranial nerve) motor neuron migration and for axon pathfinding of trigeminal (Vth cranial nerve) motor axons. We show that *lzr/pbx4* is required for *Hox* paralog group 1 and 2 function, suggesting that Pbx interacts with these proteins. Consistent with this, *lzr/pbx4* interacts genetically with *hoxb1a* to control facial motor neuron migration. Using genetic mosaic analysis, we show that *lzr/pbx4* and *hoxb1a* are primarily required cell-autonomously within the facial motor neurons; however, analysis of a subtle non-cell-autonomous effect indicates that facial motor neuron migration is promoted by interactions amongst the migrating neurons. At the same time, *lzr/pbx4* is required non-cell-autonomously to control the pathfinding of trigeminal motor axons. Thus, Pbx/Hox can function both cell-autonomously and non-cell-autonomously to direct different aspects of hindbrain motor neuron behavior.

Keywords: Pbx; Hox; Branchiomotor neurons; Neuronal migration; Zebrafish

Introduction

The transient segmentation of the hindbrain into morphologically and molecularly distinct rhombomeres is a highly conserved process in vertebrate development (Keynes and Lumsden, 1990; Gilland and Baker, 1993). Hindbrain segmentation is also illustrated by the organization of specific classes of neurons, including the cranial motor neurons (Hanneman et al., 1988; Trevarrow et al., 1990; Lumsden and Keynes, 1989). Each rhombomere has a distinct complement of motor neurons with identities and behaviors specific to their anterior/posterior position in the hindbrain. These include the branchiomotor neurons that innervate the pharyngeal arch musculature. The motor neurons of the trigeminal nerve (nV) are generally clustered in rhombomeres (r) 2 and r3 and project together from an r2 exit point to innervate the muscles of the mandibular arch (Lumsden and Keynes, 1989; Chandrasekhar et al., 1997). The motor neurons of the facial nerve (nVII) are specified in r4, but their final position varies in different vertebrate species. In zebrafish, they migrate posteriorly along a medial path, then migrate laterally to take up residence in r6 and r7 (Chandrasekhar et al., 1997; Higashijima et al., 2000); these neurons migrate only as far as r6 in the mouse (Auclair et al., 1996; Studer et al., 1996), and only a small number are located medially in r5 of the chick (Lumsden and Keynes, 1989; Jacob and Guthrie, 2000). Facial motor axons project from r4 to innervate muscles of the hyoid arch, forming the characteristic "genu" in fish and mice (Chandrasekhar et al., 1997; Auclair et al., 1996; Studer et al., 1996).

Correlating with the segmentation of the hindbrain is the expression of the anterior *Hox* genes [paralogous groups

* Corresponding author. Fax: +1-206-667-3308.
E-mail address: cmoens@fhcrc.org (C. Moens).

0012-1606/03/$ – see front matter © 2003 Elsevier Science (USA). All rights reserved.
PII: S0012-1606(02)00018-0

(PG) 1–4] (Wilkinson et al., 1989; Hunt et al., 1991; Prince et al., 1998). Anterior expression limits of these *Hox* genes correspond to rhombomere boundaries, and loss-of-function analyses in the mouse and zebrafish have shown that *Hox* genes play a critical role in the specification of rhombomere identities, including aspects of branchiomotor neuron development. For example, the loss of *Hoxb1* function alters the fate specification of cells located in r4 resulting in the aberrant behavior of the facial motor neurons; these cells fail to migrate posteriorly into r5 and r6 and subsequently die (Goddard et al., 1996; Studer et al., 1996). In the zebrafish, morpholino knock-down of *hoxb1a*, the functional counterpart of mouse *Hoxb1*, also prevents facial motor neuron migration; however, these unmigrated neurons survive to innervate their appropriate targets in the second branchial arch (McClintock et al., 2002). Loss-of-function of mouse *Hoxa2* results in aberrant pathfinding of the trigeminal motor nerve out of the hindbrain (Gavalas et al., 1997). All of the cells in r3 and some cells in r2 send their axons out of r4 rather than the usual r2 exit point. These data suggest that *Hox* genes play an essential role in defining specific motor neuron identities and behaviors. How do *Hox* genes control the specification and behavior of branchiomotor neurons, and where is *Hox* function needed for proper motor neuron development to occur?

The zebrafish *lazarus/pbx4* gene is a member of the TALE class of homeodomain transcription factors related to *Drosophila extradenticle*, an essential *Hox* DNA binding partner (Pöpperl et al., 2000; *exd* reviewed in Mann and Chan, 1996). Several lines of evidence indicate that *lzr/pbx4* is required for the function of multiple *Hox* genes in the zebrafish hindbrain. First, the *lzr/pbx4*$^{-/-}$ phenotype in the zebrafish mimics some *Hox* loss-of-function phenotypes in the mouse. Second, *lzr/pbx4* is required for embryos to exhibit the effects of over-expressing *hoxb2* (Pöpperl et al., 2000). Third, Lzr/Pbx4 protein binds Hoxb1b protein in vitro, and the interaction of Hoxb1b/Pbx4/Meis3 is required for the expression of *Hox* target genes (Vlachakis et al., 2000, 2001).

By examining the branchiomotor neurons of *lzr/pbx4*$^{-/-}$ embryos in the Is11-GFP transgenic line (Higashijima et al., 2000), we now demonstrate that *lzr/pbx4* is required for the normal posterior migration of facial motor neurons and for proper axon pathfinding of the trigeminal motor nerve. These phenotypes are identical to the mouse *Hoxb1* and *Hoxa2* null phenotypes, respectively. We propose that *lzr/pbx4* affects motor neuron behaviors through its effect on *Hox* gene function since the gain-of-function effects of *Hox* paralog group (PG) 1 and PG2 genes are dependent on functional *lzr/pbx4*, and the motor neuron phenotype resulting from partial loss of function of *hoxb1a* is enhanced by loss of a single copy of *lzr/pbx4*.

Previous studies of mouse mutants and mouse-chick chimeras indicated that the posterior migration of facial motor neurons is a response to guidance cues in the environment rather than entirely an intrinsic timing mechanism (Garel et al., 2000; Studer, 2001); however, what those cues are has not been established. Recently, *trilobite/strabismus*, a component of the *wnt* planar cell polarity pathway, was shown to be required autonomously and non-cell-autonomously for facial motor neuron migration in zebrafish (Bingham et al., 2002; Jessen et al., 2002). However, since other components of the PCP pathway do not affect facial motor neuron migration, the mechanism by which *tri/stb* mediates migration remains uncertain. It is also unclear how the disruption of *Hox* patterning affects this process on a cellular level. Similarly, little is known about the mechanism by which *Hox* patterning controls pathfinding of the trigeminal motor nerve. Here, we provide evidence for the nature of *hox* and *pbx* function with respect to the development and behaviors of specific neurons in the zebrafish. Using genetic mosaic analysis, we show that *lzr/pbx4* and *hoxb1a* are required cell-autonomously within the facial motor neurons for the initiation of cell migration out of r4 and into more posterior rhombomeres. Furthermore, this analysis suggests a dependence of facial motor neurons on one another for their complete migration. Finally, we show that *lzr/pbx4* functions non-cell-autonomously to control motor axon pathfinding of the trigeminal nerve.

Materials and methods

Embryos and staging

Isl1-GFP transgenic fish were a gift from Dr. S. Higashijima and Dr. H. Okamoto. The *lzr*^{b557} mutation is described in Pöpperl et al. (2000). *lzr/pbx4*$^{+/-}$; Isl1-GFP$^{tg/tg}$ adults were crossed to generate *lzr/pbx4*$^{-/-}$; Isl1-GFP$^{tg/tg}$ embryos and wild-type controls described in this study. Embryos were collected and reared at 25.5°C for stages younger than 24 h postfertilization (hpf), and at 28.5°C for older stages (Kimmel et al., 1995). In some cases, pigmentation was inhibited with phenyl-thiourea as described by Higashijima et al. (2000), and there was no detectable difference in motor neuron behavior.

Whole-mount fluorescent confocal imaging

Live embryos were mounted between two coverslips in 0.6% agarose in sterile Ringers solution. The drop of agarose was surrounded by a wall of high vacuum grease, and this chamber was filled with embryo medium containing tricaine (3-amino benzoic acidethylester) (Westerfield, 1995). Confocal images were captured as optical sections of 1.5–3 μm by using a Leica DM IRB/E microscope and the Leica TCS NT imaging software (version 1.6.587). For analysis of DiI backfilled embryos, individual focal planes from the green and red channels were overlaid to assure that filled cells were actually GFP-positive motor neurons.

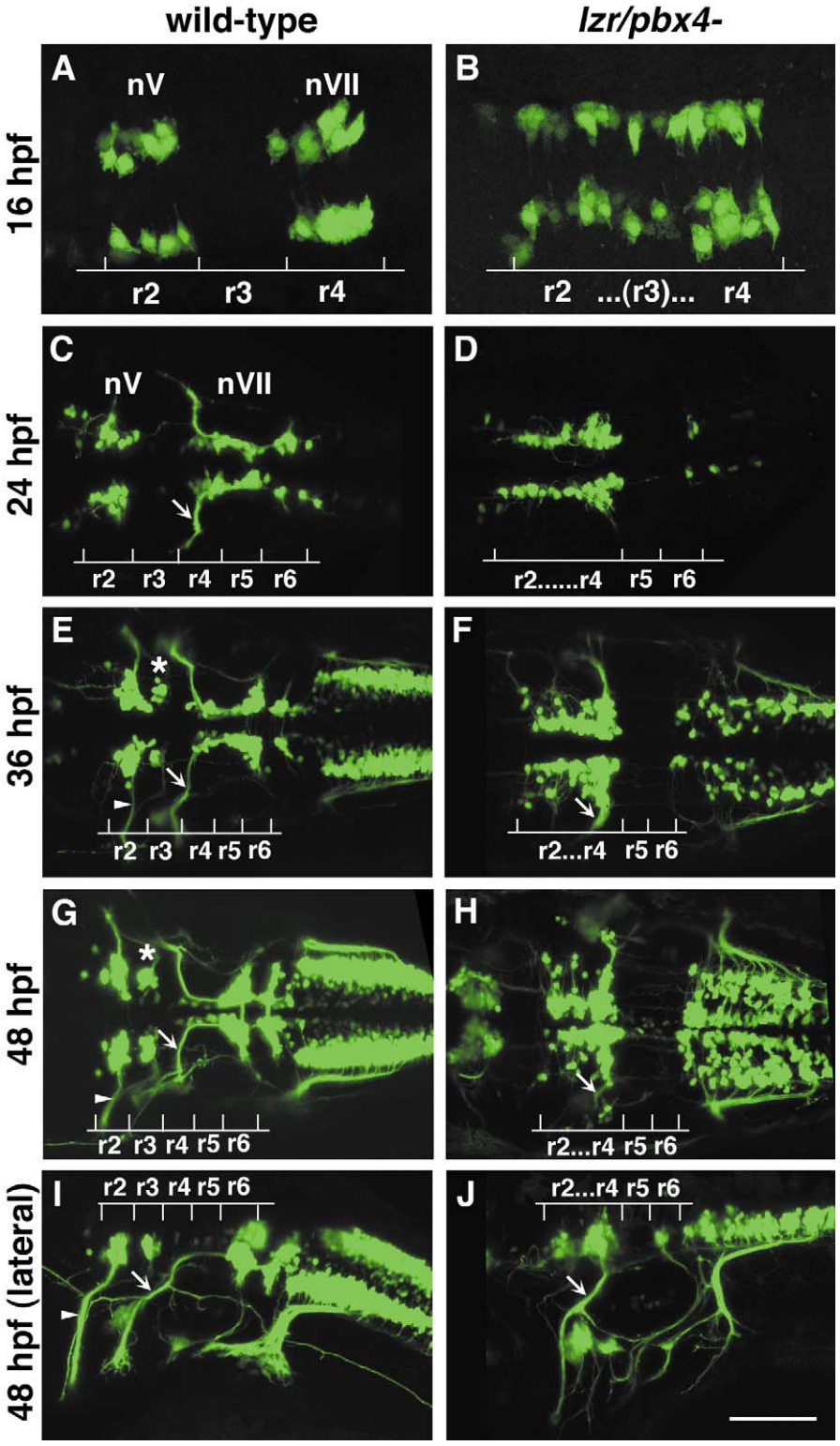

Fig. 1. Confocal images of Isl1-GFP expression in live wild-type (left column) and *lzr/pbx4*$^{-/-}$ (right column) embryos. Anterior is to the left in all panels. All images are a dorsal view, except (I) and (J) which are lateral views. (A, B) The onset of GFP expression in trigeminal (nV) motor neurons in r2 and facial (nVII) motor neurons in r4 occurs at 16 hpf. In *lzr/pbx4*$^{-/-}$ embryos, motor neurons differentiate prematurely in r3. (C, D) By 24hpf in wild-type embryos, nVII cell bodies have migrated into r5 and r6, and axons leave r4 (arrow). In *lzr/pbx4*$^{-/-}$ embryos, presumptive nVII cells have not migrated posteriorly. (E, F) nV motor neurons in r3 appear by 36 hpf in wild-type embryos (asterisk). Arrows mark the nVII motor nerve exiting in r4; arrowhead in (E) marks the nV motor nerve exiting in r2. (G, H) By 48 hpf in wild-type embryos, nVII motor neurons have completed their migration into r6 and r7, while in *lzr/pbx4*$^{-/-}$ embryos, presumptive nVII motor neurons remain in r4. Labeling is as in (E) and (F). (I, J) Lateral views of 48-hpf embryos show a strong reduction of the nV nerve (arrowhead in I) in *lzr/pbx4*$^{-/-}$ embryos accompanied by a thickening of the nVII nerve (arrow in I, J). Scale bar, 50 μm in (A) and (B); 100 μm in (C–J).

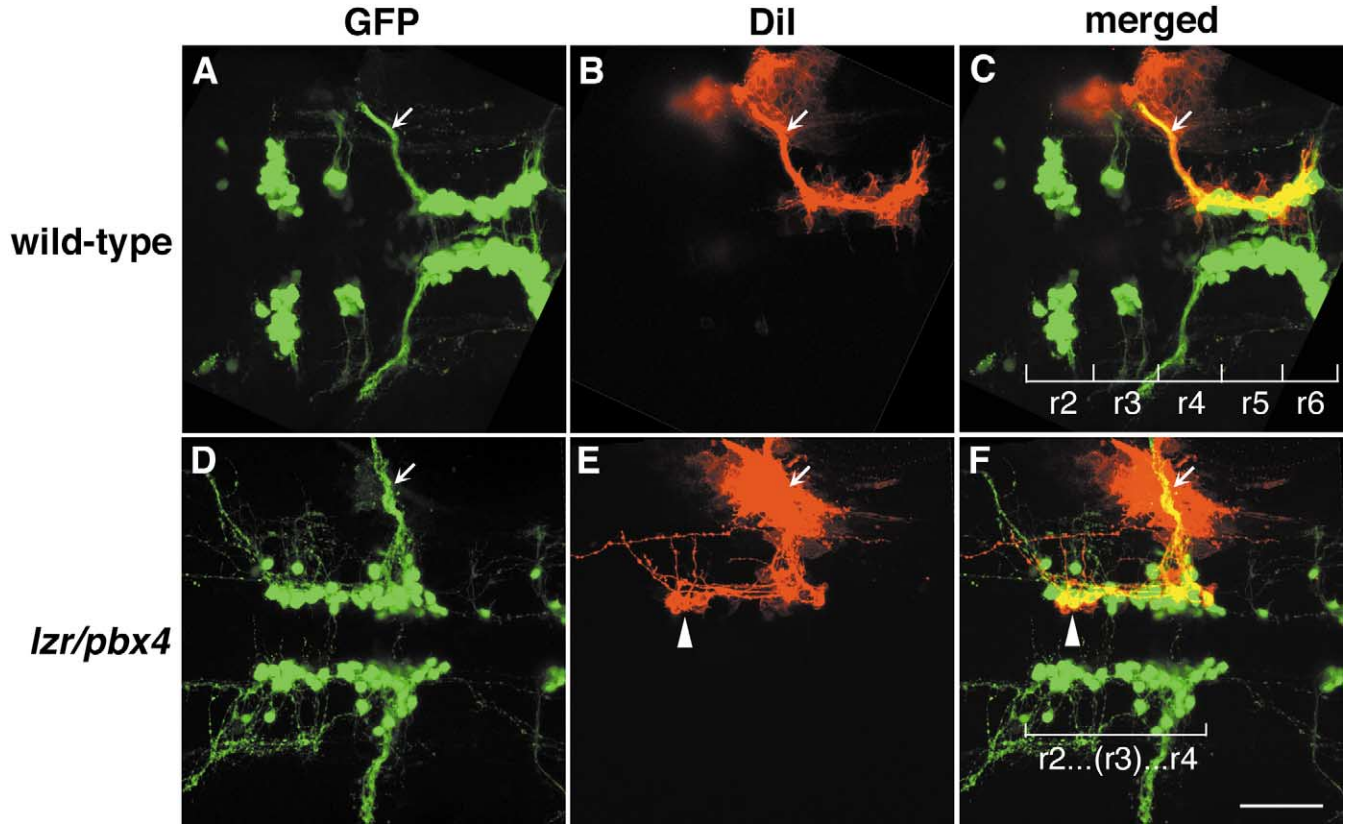

Fig. 2. Motor axons from r2 and r3 of *lzr/pbx4*$^{-/-}$ embryos misroute through the r4 exit point with the facial (nVII) nerve. Anterior is to the left in all panels. DiI was applied to the nVII nerve root distal to its r4 exit point (arrow) in fixed, 36-hpf embryos to retrogradely label nVII cell bodies within the hindbrain. (A–C) DiI fills cells located primarily in r5 and r6 of wild-type embryos. (D–F) DiI applied to the nVII root of *lzr/pbx4*$^{-/-}$ embryos fills cells in r4 as well as cells located in r2 and r3 (arrowhead in E and F). Scale bar, 50 μm.

RNA injections

hoxb1a and *hoxb1b* expression constructs are described in McClintock et al. (2001). A similar *hoxa2* expression construct was generated by cloning full-length *hoxa2* cDNA into the pCS2+ expression vector (Turner and Weintraub, 1994). Synthetic capped mRNAs were generated from linearized DNA by using the Ambion mMESSAGE mMACHINE SP6 kit following manufacturer's instructions. RNA was injected into dechorionated 1- to 2-cell-stage embryos. Wild-type and *lzr/pbx4*$^{-/-}$ embryos were sorted at 18 somites, based on morphology (Pöpperl et al., 2000). In situ hybridization was performed by using either digoxygenin- or fluorescein-labeled probes as in Prince et al. (1998). In cases where embryos could not be unambiguously sorted, they were individually genotyped as in Pöpperl et al. (2000), following in situ hybridization and analysis.

Morpholino injections

To test for a genetic interaction between *lzr/pbx4* and *hoxb1a,* 2 ng or 200 pg of *hoxb1a* morpholino or 2 ng of a *hoxb1a* mutant control morpholino (McClintock et al., 2002) was injected into one- to four-cell-stage embryos from *lzr/pbx4*$^{+/-}$*;* isl1-GFP fish crossed to *lzr/pbx4*$^{+/+}$*;* isl1-GFP. These embryos were first sorted based on GFP expression at 36 hpf into two classes: "migrated," which had facial motor neurons posterior to r4, and "unmigrated," in which all facial motor neurons were restricted to r4. Sorted embryos were genotyped to distinguish between *lzr/pbx4*$^{+/-}$ and *lzr/pbx4*$^{+/+}$ individuals as previously described (Pöpperl et al., 2000). The significance of the tendency of *lzr/pbx4*$^{+/-}$ individuals to be in the unmigrated class and of *lzr/pbx4*$^{+/+}$ individuals to be in the migrated class was determined by a Chi-Square Test.

Mosaic analysis

Donors were labeled with rhodamine dextran and biotin dextran (2.5% each in 0.2 M KCl). Cells were transplanted to shield stage hosts (Moens and Fritz, 1999) from donor embryos of a homozygous Isl1-GFP$^{tg/tg}$; *lzr/pbx4*$^{+/-}$ intercross. Host embryos were nontransgenic *lzr/pbx4*$^{+/-}$ intercross progeny. Cells were targeted to the region adjacent to the shield approximately one-third of the distance from the margin to the animal pole so that donor-derived cells would

be restricted to the ventral neural tube, including the anterior hindbrain (Woo and Fraser, 1995).

Host embryos were photographed at 36 hpf, a time at which migration is still in progress, and a migration score was calculated as a weighted average of the number of cells in each rhombomere. Letting the number of cells reaching each rhombomere be represented by r4, r5, r6, and r7, respectively, the migration score (MS) was calculated by using the following formula: MS = (r5/2 + r6 + r7)/(total number of wild-type donor facial motor neurons per embryo). The term "r5/2" was chosen because cells in r5 are neither unmigrated nor fully migrated, but rather approximately half-way to their final location. The comparison of mean migration scores and the relationship between the number of wild-type cells transplanted and the migration score were both evaluated by using weighted linear regression with robust variance estimates to account for heteroskedasticity of the data (White, 1980). Statistical tests to compare mean migration scores, tests of whether the slopes of the relationship between MS and number of wild-type donor cells were significantly different from zero and the comparison of slopes between wild-type, *lzr/pbx4*$^{-/-}$ and *hoxb1aMO* hosts were carried out by comparing coefficients from the relevant regression models. All statistical tests were two-sided and considered significant at the 0.05 level.

Results

lazarus/pbx4 is required for the proper behavior of branchiomotor neurons

The organization of branchiomotor neurons in the zebrafish hindbrain has been described previously (Chandrasekhar et al., 1997; Higashijima et al, 2000). We examined the organization and behavior of branchiomotor neurons in live, Isl1-GFP transgenic (Higashijima et al., 2000), wild-type and *lzr/pbx4*$^{-/-}$ embryos by time-lapse confocal microscopy. Wild-type branchiomotor neurons begin to express Isl1-GFP at 16 hpf in distinct clusters of trigeminal (nV) motor neurons located in r2 and facial (nVII) motor neurons located in r4 (Fig. 1A). Twenty hours later, at about 36 hpf, the r3 cluster of trigeminal motor neurons begins to express GFP (Fig. 1E). This is consistent with work in the chick that suggests that motor neurons in even numbered rhombomeres differentiate earlier than neurons in odd numbered rhombomeres (Lumsden and Keynes, 1989). The cell bodies of the trigeminal motor nerve migrate laterally within r2 and r3, and the axons exit from r2 to extend into the first (mandibular) arch (Fig. 1G and I). By 19 hpf, the facial motor neurons in r4 initiate their caudal migration into r5 and r6, and by 36 hpf, they begin to establish lateral clusters in r6 and r7 (Fig. 1E). As the cell bodies migrate from r4, they leave axons behind them that exit the hindbrain from r4 at 24 hpf (Fig. 1C) to ultimately innervate muscles of the second (hyoid) arch.

In 16-hpf *lzr/pbx4*$^{-/-}$ embryos, a continuous line of cells with no obvious segmentation differentiates in the region of r2 through r4 (Fig. 1B). None of these cells migrate in the anterior/posterior axis, and presumptive facial motor neurons are still located in r4, having failed to migrate from their birthplace into more posterior rhombomeres, as late as 6–7 days postfertilization (dpf) when the embryos die of multiple defects (data not shown). Cell bodies in r4 migrate laterally by 36 hpf, while the majority of cells located more anteriorly in r2 and r3 remain medial throughout development (Fig. 1F). These data are consistent with the ectopic expression of *tag-1* in r4 neurons of 36-hpf *lzr/pbx4* embryos (Pöpperl et al., 2000). In addition, the motor nerve projection from r2 appears reduced or missing entirely, and axons from cells located in r2 and r3 project unfasiculated to the lateral edge of the hindbrain where they terminate. These axon defects are often accompanied by a thickening of the motor nerve exiting r4 (Fig. 1F).

lzr/pbx4$^{-/-}$ *embryos display axon pathfinding defects of the presumptive trigeminal motor neurons*

We hypothesized that the reduction of the trigeminal nerve and thickening of the facial nerve results from motor neurons in r2 and r3 that improperly contribute axons to the facial nerve. However, the dense clustering of GFP-positive cell bodies in r2 through r4 obscures the visualization of axons in the hindbrain. To address this hypothesis, we performed retrograde labeling of cell bodies located in the hindbrain by applying DiI to the nerve exiting r4 in 36-hpf fixed embryos (Chandrasekhar et al., 1997). In wild-type embryos, such an application of DiI labels cell bodies of facial motor neurons that are located primarily in r5 and r6 at this stage (Fig. 2A–C; $n = 9$). In *lzr/pbx4*$^{-/-}$ embryos, application of DiI to axons leaving from r4 labels cell bodies located in r4 and often cells located more anteriorly in r3 and even r2 but rarely r5 and never r6 (Fig. 2D–F; $n = 8$). Thus, *lzr/pbx4* is required both for the posterior migration of presumptive facial motor neurons and for the accurate pathfinding of trigeminal motor axons from r2. In the absence of *lzr/pbx4* function, few trigeminal axons exit the hindbrain at the level of r2, but instead project together with the facial motor axons from the r4 exit point.

lzr/pbx4 is required for effects of Hox over-expression

The branchiomotor neuron phenotypes described here in *lzr/pbx4*$^{-/-}$ embryos closely resemble *Hoxb1* and *Hoxa2* loss-of-function phenotypes in the mouse. In the *Hoxb1* null mouse, facial motor neurons fail to migrate posterior to r4 (Goddard et al., 1996; Studer et al., 1996), while in the *Hoxa2* null mouse, all of the r3 and some of the r2 trigeminal motor neurons send axons from r4 with the facial nerve (Gavalas et al., 1997). Since *lazarus* is a member of the *Pbx* family of essential *Hox* DNA binding partners (Pöpperl et al., 2000), we hypothesize that the branchiomotor neuron phenotypes described in *lzr/pbx4*$^{-/-}$ embryos are due to the

loss of *Hox* function. To test this, we began by examining the requirement of *lzr/pbx4* for aspects of *hox* gene function. We have previously shown that *lzr/pbx4* is required for the effects of over-expression of one paralog group 2 (PG2) gene, *hoxb2* (Pöpperl et al., 2000). We tested whether *lzr/pbx4* is similarly required for the effects of another PG2 gene, *hoxa2*, and the zebrafish *hoxb1* paralogs.

In the fish, there are two paralogs of *hoxb1*: *hoxb1a* and *hoxb1b* (Amores et al., 1998; McClintock et al., 2001, 2002). The effects of over-expressing *Hox* PG1 genes in wild-type zebrafish embryos have been described previously (McClintock et al., 2001). Injection of approximately 80 pg of *hoxb1a* mRNA into wild-type embryos results in ectopic expression in r2 of endogenous *hoxb1a*, which is normally restricted to r4 (Fig. 3C). Injecting the same amount of *hoxb1a* mRNA into *lzr/pbx4*$^{-/-}$ embryos, on the other hand, does not cause this phenotype, demonstrating that *lzr/pbx4* is required for the full effects of *hoxb1a* over-expression (Fig. 3D). A total of 200 pg of *hoxb1a* injected into wild-type embryos has broader effects, driving ectopic expression of endogenous *hoxb1a* in the midbrain, forebrain, and the eyes in addition to r2 (Fig. 3E). This amount of *hoxb1a* injected into *lzr/pbx4*$^{-/-}$ embryos causes expression of endogenous *hoxb1a* in r2 but not in the midbrain, forebrain, or eyes (Fig. 3F), resembling the phenotype caused by injection of 80 pg of *hoxb1a* mRNA into wild-type embryos. *krox20* expression in r3 is also variably expanded in wild-type and *lzr/pbx4*$^{-/-}$ embryos injected with *hoxb1a* mRNA. Thus, eliminating zygotic *lzr/pbx4* function strongly suppresses, but does not entirely block, the effects of ectopic *hoxb1a.*

Similarly, the effects of ectopic *hoxb1b* and *hoxa2* expression are also suppressed in *lzr/pbx4*$^{-/-}$ embryos. Like *hoxb1a*, ectopic *hoxb1b* causes expression of endogenous *hoxb1a* in r2 (Fig. 3G; McClintock et al., 2001). This phenotype is not observed in *lzr/pbx4*$^{-/-}$ embryos (Fig. 3H), although a variable expansion of *krox20* expression in r3 is observed in wild-type and *lzr/pbx4*$^{-/-}$ embryos injected with *hoxb1b.* Ectopic *hoxa2* induces *krox20* expression in the eye (Fig. 3I), similar to the effects of *hoxb1a* (Fig. 3C) and *hoxb2* over-expression (Yan et al., 1998; Pöpperl et al., 2000). This phenotype is observed at a much lower frequency in *lzr/pbx4*$^{-/-}$ embryos [Fig. 3J; 91% of wild-type embryos ($n = 65$) vs 24% of *lzr/pbx4*$^{-/-}$ embryos ($n = 21$)]. From these results, we conclude that the absence of zygotic *lzr/pbx4* function strongly suppresses the effects of ectopic *Hox* PG1 and PG2 expression, and therefore *lzr/pbx4* is required for full function of these *Hox* genes. The presence of maternal *lzr/pbx4* product and/or products of other *Pbx* genes expressed in the embryo may explain why this effect is not complete (see Discussion).

lzr/pbx4 functions with hoxb1a to control facial motor neuron migration

The above gain-of-function experiments suggest that *lzr/pbx4* is required for *Hox* PG1 and PG2 gene function. A morpholino antisense oligonucleotide (Nasivicius and Ekker, 2000) designed to knock-down *hoxb1a* function prevents facial motor neuron migration (Fig. 4B; McClintock et al., 2002), a phenotype equivalent to the facial motor neuron phenotypes of *lzr/pbx4*$^{-/-}$ zebrafish and *Hoxb1* null mice (Studer et al., 1996; Goddard et al., 1996). The phenotypic similarities and the requirement of *lzr/pbx4* for full *hoxb1a* function, together with the known in vitro interaction between Pbx4 and Hox PG1 proteins (Vlachakis et al., 2000) led us to hypothesize that an interaction between Lzr/Pbx4 and Hoxb1a is required for normal facial motor neuron development. To confirm such an interaction genetically, we employed an assay using subthreshold amounts of the *hoxb1a* morpholino in combination with loss of one copy of *lzr/pbx4* to create a synthetic phenotype in injected, heterozygous embryos.

Injecting 2 ng of *hoxb1a* morpholino prevents the migration of presumptive facial motor neurons posterior from r4 in 95% ($n = 62$) of wild-type embryos (Fig. 4B). We tested the interaction of *hoxb1a* and *lzr/pbx4* by injecting a near-threshold dose (200 pg) of this morpholino into embryos from a *lzr/pbx4*$^{+/-}$ × *lzr/pbx4*$^{+/+}$ cross. Fifty-eight percent of *lzr/pbx4*$^{+/-}$ embryos injected with 200 pg *hoxb1a* morpholino exhibited a facial motor neuron migration defect, compared with 23% of *lzr/pbx4*$^{+/+}$ embryos (Fig. 4E). Only 1–1.5% of uninjected or control morpholino-injected *lzr/pbx4*$^{+/-}$ embryos ever exhibit this phenotype (Fig. 4A and E). This degree of deviation is unlikely to be due to random chance ($P \leq 0.01$) and demonstrates that reducing both *hoxb1a* and *lzr/pbx4* function creates a synthetic phenotype indicative of a strong genetic interaction between these two genes. This interaction supports the hypothesis that the defect in facial motor neuron migration in *lzr/pbx4*$^{-/-}$ embryos is due to the loss of Hoxb1a activity in the absence of its required DNA binding partner.

lzr/pbx4 is required both autonomously and nonautonomously to control different aspects of branchiomotor neuron behavior

Our above results show that *lzr/pbx4* functions with *hoxb1a* to control facial motor neuron migration, and also functions, possibly in a *Hox*-dependent manner, to control axon pathfinding of the presumptive trigeminal motor nerve. Where does Lzr/Pbx4, with its partners, function to promote correct motor neuron behaviors in wild-type embryos? The classical function of *Hox* genes is to specify segment identity, and *lzr/pbx4*, which is expressed ubiquitously, may function together with specific *Hox* genes within the motor neurons to confer their regional identities. Acquiring these appropriate identities would in turn allow trigeminal neurons to respond to signals that direct their axons into the first arch, and would allow facial motor neurons to respond to signals that direct their caudal migration. However, it is also possible that Lzr/Pbx4 functions outside the motor neurons to control these behaviors, for

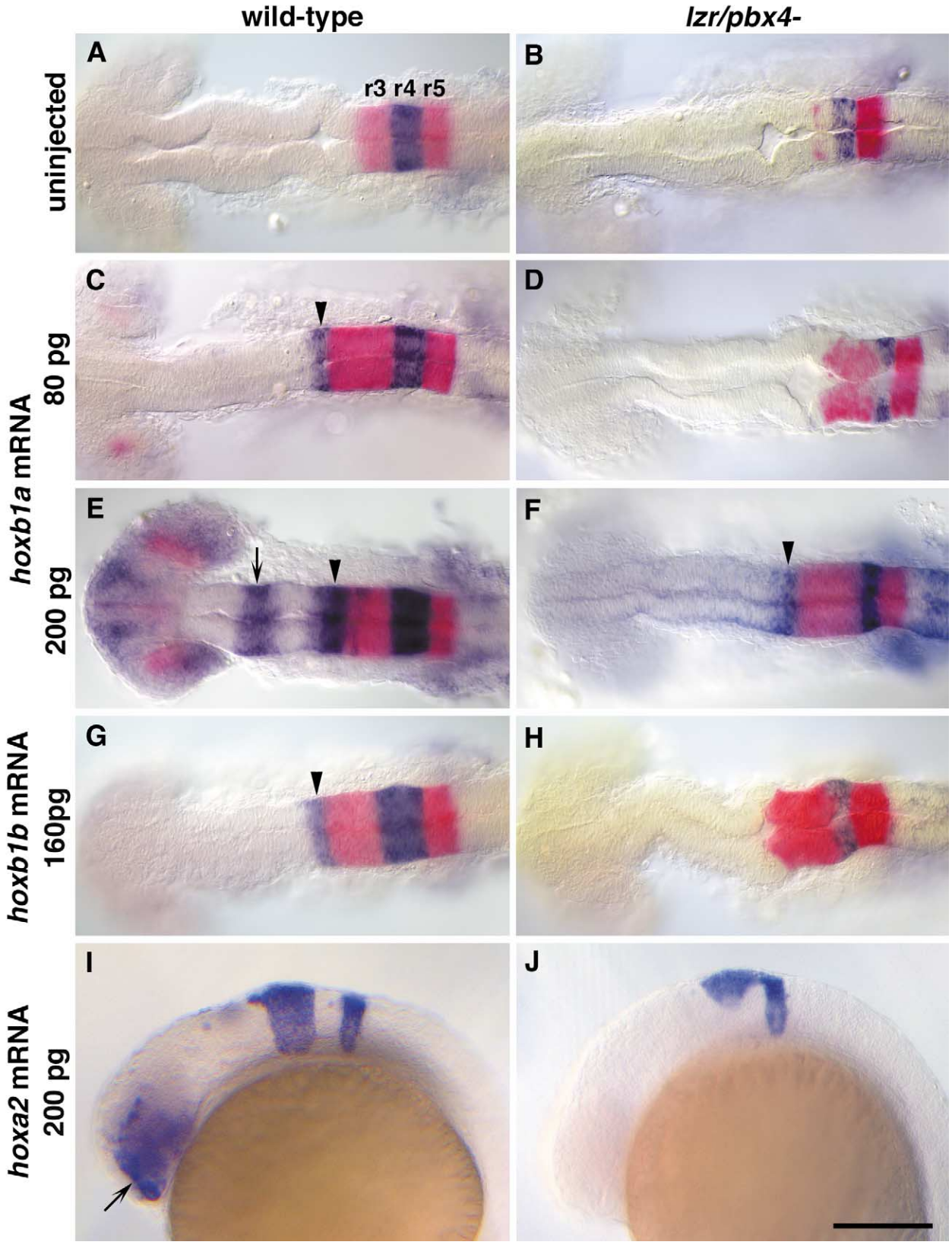

Fig. 3. *lazarus/pbx4* is required for the ectopic effects of *hoxb1a*, *hoxb1b*, and *hoxa2*. RNA in situ hybridization with *krox20* (red in A–H, blue in I, J) and *hoxb1a* (blue in A–H) on wild-type (left column) and *lzr/pbx4*$^{-/-}$ (right column) embryos treated as shown. (A, B) In uninjected embryos, *krox20* is expressed in r3 and r5, and *hoxb1a* is expressed in r4. In *lzr/pbx4*$^{-/-}$ embryos, *krox20* expression in r3 and *hoxb1a* expression in r4 are reduced. (C–F) The effects of ectopically expressing *hoxb1a* at 80 (C, D) and 200 pg (E, F) are suppressed in *lzr/pbx4*$^{-/-}$ embryos. Arrowheads and arrows indicate ectopic endogenous *hoxb1a* expression in r2 and in the midbrain, respectively. (G, H) Similarly, the effects of over-expressing *hoxb1b* at about 160 pg are suppressed in *lzr/pbx4*$^{-/-}$ embryos. (I, J) Ectopic *hoxa2* expression (200 pg) results in *krox20* expression in the eyes of wild-type embryos (arrow in I), and this effect is also suppressed in *lzr/pbx4*$^{-/-}$ embryos. Scale bar, 100 μm in (A–H); 200 μm in (I) and (J).

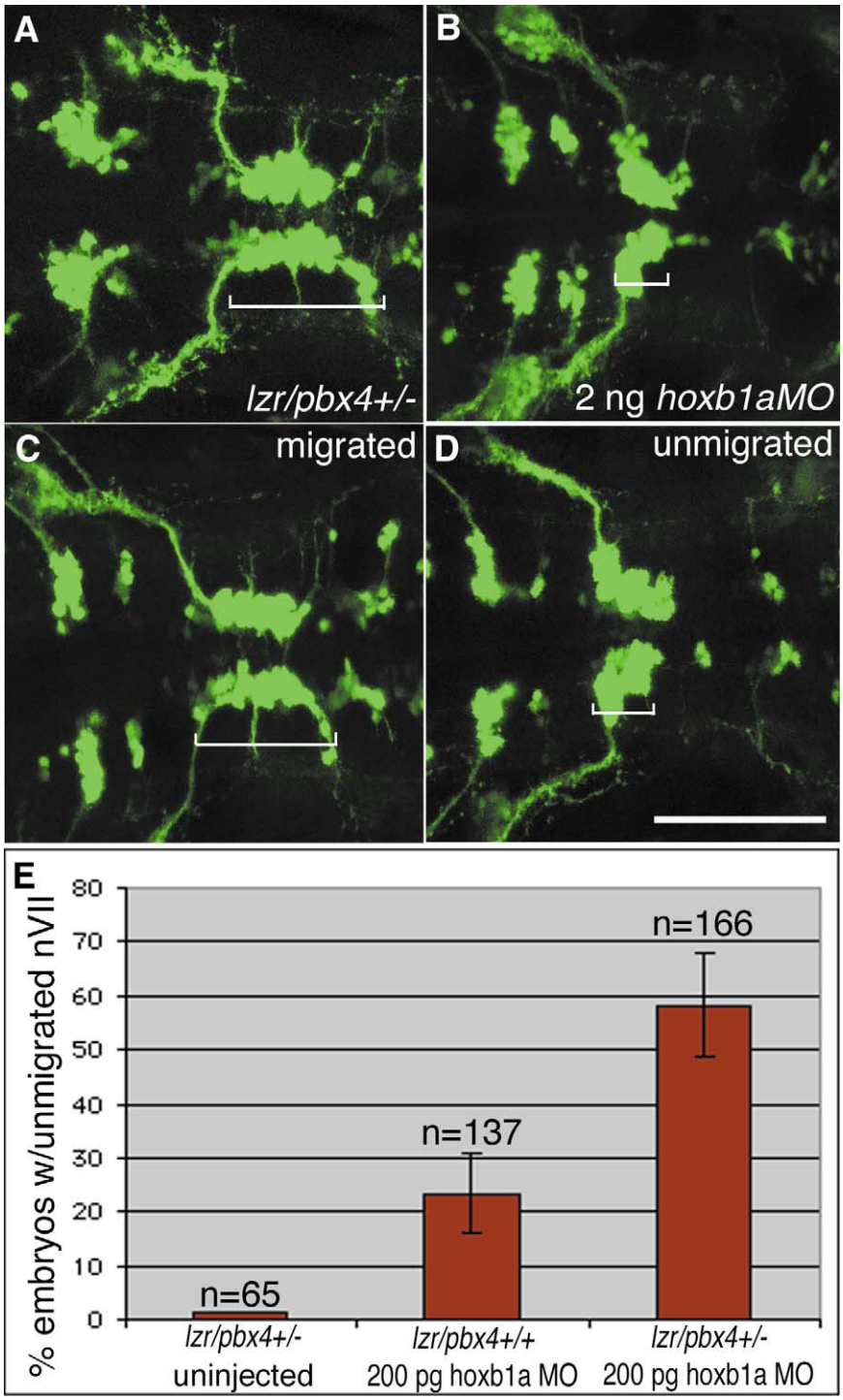

Fig. 4. Loss of one copy of *lazarus/pbx4* enhances effects of *hoxb1a* morpholinos on nVII motor neuron migration. (A–D) Confocal images of live embryos at 36 hpf. Brackets indicate the positions of facial (nVII) motor neurons in each panel. (A) *lzr/pbx4*$^{+/-}$ facial motor neurons migrate normally as in *lzr/pbx4*$^{+/+}$ embryos (see Fig. 1E). (B) A total of 2 ng of *hoxb1aMO* blocks presumptive facial motor neuron migration in 95% of injected, *lzr/pbx4*$^{+/+}$ embryos. (C, D) Classes of phenotypes observed after injecting 10-fold less (200 pg) *hoxb1a* morpholino: (C) "migrated" and (D) "unmigrated." (E) A summary of the average percentage of *lzr/pbx4*$^{+/+}$ and *lzr/pbx4*$^{+/-}$ embryos with unmigrated r4-derived motor neurons following injection of 200 pg *hoxb1aMO*. Error bars represent standard deviations across five independent experiments. The value "*n*" indicates the total number of embryos represented in these experiments. Chi-square tests on data from individual experiments demonstrate statistical significance to the differences observed between *lzr/pbx4*$^{+/+}$ and *lzr/pbx4*$^{+/-}$ embryos ($P < 0.01$). Scale bar, 100 μm.

example, to regulate the expression of signals that attract or repel axon outgrowth or neuronal migration. To address these questions, we generated genetic mosaics in which the genotype of the branchiomotor neurons differed from that of their surroundings. In these experiments, cells were transplanted from isl1-GFP transgenic donors labeled with rho-

damine dextran lineage tracer into the presumptive ventral hindbrain of nontransgenic host embryos at the early gastrula stage (Fig. 5A). Donor-derived cells contribute consistently to the ventral hindbrain, including the branchiomotor neurons.

When cells are transplanted between wild-type embryos at the gastrula stage, they contribute uniformly to the ventral hindbrain, and donor-derived trigeminal and facial motor neurons develop and behave normally (Fig. 5B; $n = 70$ embryos). Thus, trigeminal motor neurons appear in r2 and r3 and project axons laterally from r2, while facial motor neurons migrate posteriorly into r6 and r7 and project axons out of lateral r4. When *lzr/pbx4*$^{-/-}$ motor neurons are present in r2 and r3 of a wild-type host, the axons always pathfind normally out of the r2 trigeminal exit point (Fig. 5C; $n = 22$ embryos). Conversely, axons of wild-type trigeminal motor neurons transplanted into a *lzr/pbx4*$^{-/-}$ host embryo often misroute (in 69% of hosts), exiting the hindbrain from r4 together with the facial motor nerve (Fig. 5D; $n = 35$ embryos). Axons either project posteriorly along a medial path to exit from r4 or project first to the lateral edge of the hindbrain, then turn posteriorly to join the nerve exiting r4. Together, these results show that *lzr/pbx4* functions non-cell-autonomously to control trigeminal motor axon pathfinding.

In contrast, the behavior of facial motor neurons in genetic mosaics is consistent with a cell-autonomous role for *lzr/pbx4* in controlling their migration. Wild-type facial motor neurons transplanted into a *lzr/pbx4*$^{-/-}$ host embryo initiate migration and are distributed throughout r4-7 by 36 hpf (Fig. 5D; 21/30 embryos), although they migrate less completely than in a wild-type host (see below). Since, in this experiment, it is possible that the small population of donor-derived nonmotor neurons within the mutant hindbrain (red cells in Fig. 5D) could provide non-autonomous signals that induce the wild-type facial motor neurons to migrate, we analyzed the reciprocal transplant. *lzr/pbx4*$^{-/-}$ motor neurons fail to migrate posteriorly from r4 in a wild-type host and are very rarely seen in more posterior rhombomeres (Fig. 5C; no migration in 21/22 embryos). Unmigrated *lzr/pbx4*$^{-/-}$ facial motor neurons persist in this position until at least 4.5 dpf, well after the host facial motor neurons have completed their migration (data not shown). Together, these reciprocal experiments indicate that *lzr/pbx4* function is required cell-autonomously within facial motor neurons for their posterior migration.

hoxb1a is required cell-autonomously to control facial motor neuron migration

We have shown that the *lzr/pbx4*$^{-/-}$ and *hoxb1a MO* facial motor neuron phenotypes are identical, and that *lzr/pbx4* and *hoxb1a* interact genetically to control facial motor neuron migration. Since the mosaic analysis described above demonstrates a cell-autonomous requirement for *lzr/pbx4* in facial motor neuron migration, we addressed whether a similar role can be attributed to *hoxb1a* function. We generated genetic mosaic embryos where the donor or host embryos were injected with 2 ng of *hoxb1aMO*. We found that all *hoxb1aMO* donor cells placed in a wild-type host embryo fail to migrate posterior from r4 in 66% of hosts (Fig. 5E; 23/35 embryos). In the reciprocal transplant, wild type facial motor neurons in a *hoxb1aMO*-injected host do migrate from r4 to populate r4–r7 by 36 hpf (Fig. 5F; 82%, 45/55 embryos), indicating that, like *lzr/pbx4*, *hoxb1a* is required autonomously for facial motor neuron migration.

A non-cell-autonomous effect of hoxb1a and lzr/pbx4 is attributable to a "community effect" of migration

In our analysis, we noted that the distribution of wild-type donor-derived facial motor neurons migrated farther in wild-type hosts than in either *hoxb1aMO* or *lzr/pbx4*$^{-/-}$ hosts (Fig. 6A). Comparison of mean migration scores between wild-type and *hoxb1aMO* or *lzr/pbx4*$^{-/-}$ hosts also indicated significant differences ($P = 0.002$ and $P < 0.001$, respectively), suggesting an apparent non-cell-autonomous requirement for the function of these genes. One possibility is that the region through which facial motor neurons migrate, which has been shown to provide migratory cues (Studer, 2001), is patterned abnormally in *lzr/pbx4* and *hoxb1aMO* embryos. However, careful analysis of gene expression patterns in r4–r7 did not reveal any such patterning defects in *hoxb1aMO* embryos (data not shown) and revealed only a subtle narrowing of the r5/6 domain in *lzr/pbx4* mutants (Pöpperl et al., 2000).

Another possibility is that there is a "community effect" to migration (Gurdon et al., 1993; Yang et al., 1993), such that while facial motor neurons can exit r4 independently, interactions between migrating motor neurons promote their migration. Since the endogenous motor neurons in *hoxb1aMO* and *lzr/pbx4*$^{-/-}$ hosts do not migrate, wild-type donor-derived facial motor neurons must migrate singly or in small numbers. We plotted the calculated migration score for each embryo (see Materials and methods) vs the number of donor-derived motor neurons per embryo and fit weighted linear regression analyses to evaluate the degree to which the migration score increases with the number of donor motor neurons per embryo (Fig. 6B–D). The slope of the regression line for wild-type cells in *lzr/pbx4*$^{-/-}$ hosts and *hoxb1aMO* hosts is significantly greater than zero ($P = 0.01$ and $P < 0.001$, respectively; Fig. 6C and D), illustrating a positive correlation between number of cells and extent of migration and providing evidence for a "community effect" amongst migrating facial motor neurons. In contrast, the slope for wild-type cells in wild-type hosts, where the host motor neurons migrate, is not significantly greater than zero (Fig. 6B). We note, however, that the observed correlation between distance of migration and number of migrating motor neurons does not eliminate the possibility that donor-derived non-motor neurons included in the transplant (red cells in Fig. 5D and F) may also

promote wild-type facial motor neuron migration in these mosaic embryos.

We also note that, while the slopes of the regression lines for wild-type cells migrating in *lzr/pbx4*$^{-/-}$ hosts vs *hoxb1aMO* hosts do not significantly differ ($P = 0.46$), wild-type cells in a *hoxb1aMO* host migrate significantly farther than cells in a *lzr/pbx4* mutant ($P = 0.009$). This suggests that perhaps *lzr/pbx4* has an additional non-cell-autonomous role in facial motor neuron migration that is independent of its function with *hoxb1a*, possibly attributable to the subtle effect that *lzr/pbx4* and not *hoxb1a* has on caudal hindbrain patterning.

Discussion

We have determined that presumptive facial motor neurons (nVII) in *lzr/pbx4*$^{-/-}$ embryos fail to migrate posterior from r4, while trigeminal motor axons (nV) misroute through the r4 exit point with the facial motor nerve, resembling the branchiomotor neuron phenotype of the *Hoxb1* and *Hoxa2* null mouse, respectively. Using *Hox* gain-of-function approaches, we have found that *lzr/pbx4* is required for the full function of two *hoxb1* paralogs, *hoxb1a* and *hoxb1b*, and for the function of *hoxa2*. We also determined that partial loss of both *lzr/pbx4* and *hoxb1a* function generates a synthetic motor neuron phenotype, confirming that *lzr/pbx4* functions with *hoxb1a* to control aspects of facial motor neuron development. Through genetic mosaic analysis, we found that *lzr/pbx4* and *hoxb1a* function primarily in a cell-autonomous manner to promote facial motor neuron migration from r4 into more posterior rhombomeres. Further analysis also uncovers a subtle non-cell-autonomous effect in mosaics that indicates that facial motor neurons depend on homotypic cell–cell interactions for thorough migration. In contrast, the ability of trigeminal motor axons to pathfind correctly to their r2 exit point is not dependent on *lzr/pbx4* function in the individual neurons themselves, but rather on non-autonomous *lzr/pbx4* function in other cells of the hindbrain or head periphery.

lzr/pbx4 and hoxb1a interact to control facial motor neuron migration

The gain-of-function data presented here provide further support for previous data, showing that Pbx proteins function as DNA binding partners for vertebrate Hox paralog group 1 (PG1) proteins. In the mouse, *Hoxa1* and *Hoxb1* each bind to sites for an essential *Hox/Pbx* element in the enhancer of *Hoxb1* (Pöpperl et al., 1995; Studer et al., 1998). In the zebrafish, Lzr/Pbx4, Hoxb1b, and Meis3 bind in vitro, and this interaction is required for the effects of ectopic *hoxb1b* (Vlachakis et al., 2000, 2001). We show here that zygotic *lzr/pbx4* is required for some of the gain-of-function effects of *hoxb1a* and *hoxb1b*. This effect is expected to be partial since maternal *lzr/pbx4* mRNA persists until early somite stages (Pöpperl et al., 2000), and since another Pbx protein, Pbx2, partially compensates for loss of Lzr/Pbx4 in the zebrafish (Waskiewicz et al., 2002). Furthermore, loss of *lzr/pbx4* and *hoxb1a* function causes identical facial motor neuron migration phenotypes, and partial loss of both *lzr/pbx4* and *hoxb1a* function creates a synthetic facial motor neuron migration phenotype indicative of a strong genetic interaction between these two genes. Taken together, these data support the idea that *lzr/pbx4* functions together with *hoxb1a* to control facial motor neuron migration, and from this we conclude that the facial motor neuron migration defects that we observe in *lzr/pbx4*$^{-/-}$ embryos result from the inability of *hoxb1a* to function normally in the absence of *lzr/pbx4*.

In the mouse, *Hoxb1* is required for facial motor neuron migration and survival (Goddard et al., 1996; Studer et al., 1996). In the absence of *Hoxb1* function, r4 is weakly transformed to r2 identity (Studer et al., 1996), and it was hypothesized that facial motor neurons lacking *hoxb1a* fail to migrate because they are mis-specified as r2 (trigeminal-like) motor neurons, which do not normally migrate caudally. Furthermore, *Hoxb1* over-expression has been observed to transform motor neurons to facial identity (Bell et al., 1999; Jungbluth et al., 1999). We have not observed evidence of an r4-to-r2 transformation in *lzr/pbx4*$^{-/-}$ or *hoxb1aMO* zebrafish embryos, although aspects of r4 identity are lost in *lzr/pbx4* mutants (Pöpperl et al., 2000). The unmigrated facial motor neurons in *lzr/pbx4* mutants or *hoxb1a* morphants survive and innervate the appropriate targets in the second pharyngeal arch, suggesting that they have acquired at least some aspects of r4 identity (McClintock et al., 2002; data not shown). Our genetic mosaic data demonstrate that *lzr/pbx4* and *hoxb1a* are both required cell-autonomously for the migration of facial motor neurons out of r4, since *lzr/pbx4*$^{-/-}$ or *hoxb1a* morpholino-depleted motor neurons fail to migrate in a wild-type host hindbrain. This cell-autonomous function is consistent with *lzr/pbx4* and *hoxb1a* being required to specify some aspects of facial motor neuron identity, including the ability to respond to migratory cues. Thus *lzr/pbx4* and *hoxb1a* may function, directly or indirectly, to control the expression of cell surface receptors that allow facial motor neurons to respond to guidance molecules. A thorough analysis of gene expression differences between wild-type and *lzr/pbx4*$^{-/-}$ facial motor neurons will likely identify direct and indirect *Hox* targets required for autonomous aspects of the response to environmental signals.

Our genetic mosaic analysis revealed an apparent non-cell-autonomous role for both *lzr/pbx4* and *hoxb1a* in facial motor neuron migration, since wild-type facial motor neurons migrate significantly less in *lzr/pbx4* or *hoxb1a* mutant hosts than in wild-type hosts. We observed that the distance that wild-type donor-derived facial motor neurons migrate in a *lzr/pbx4* or *hoxb1a* host correlates with the total number of donor-derived motor neurons in that host, while no such correlation is observed in a wild-type host where the host

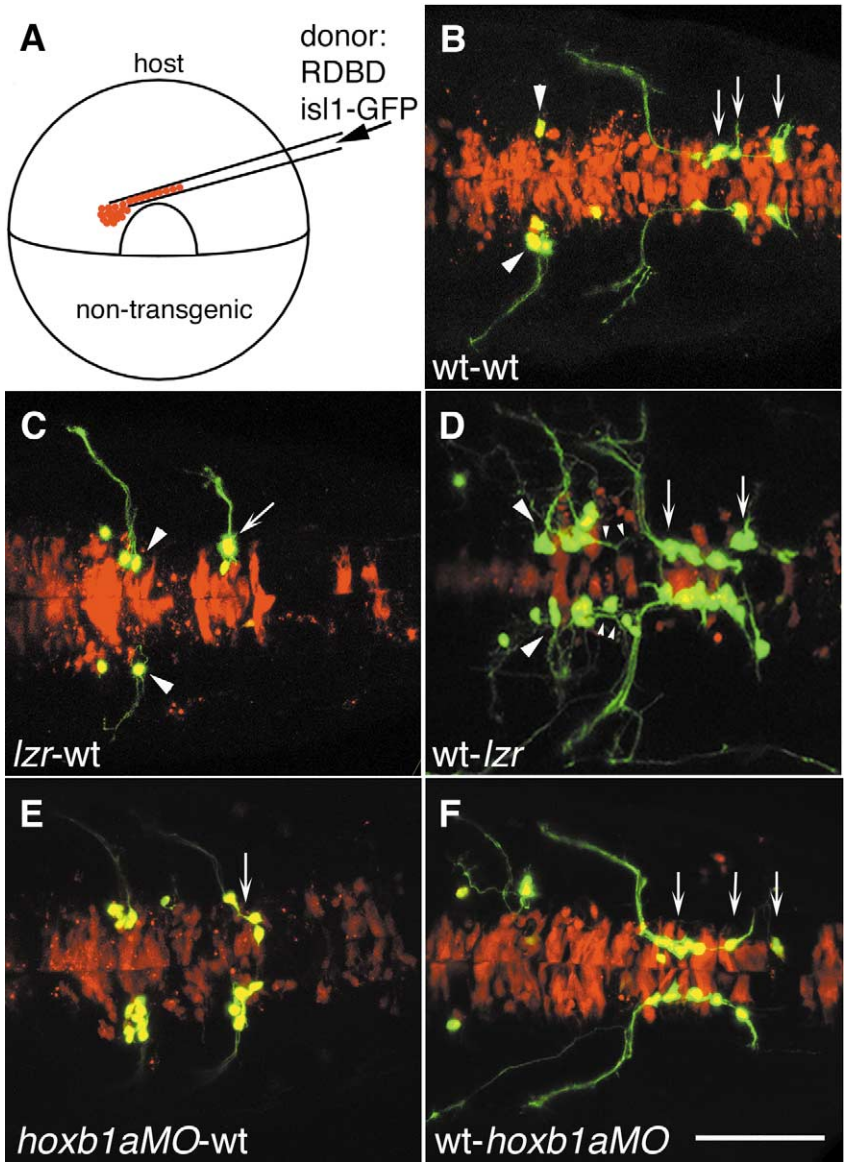

Fig. 5. *lazarus* is required non-autonomously for nV axon pathfinding, and *lazarus* and *hoxb1a* are both required autonomously for nVII motor neuron migration. (A) Schematic of experimental design: cells from a lineage-labeled transgenic donor embryo were transplanted into the presumptive ventral hindbrain of an unlabeled, nontransgenic host embryo at 6 hpf. (B–F) Confocal images of 36-hpf host embryos. Anterior is to the left. (B) Control transplant of wild-type donor cells (red, yellow if GFP-expressing) into a wild-type host, showing normal development of donor-derived branchiomotor neurons. Arrowheads: trigeminal (nV) motor neurons in r2; arrows: facial (nVII) motor neurons in r5, r6, and r7. (C) *lzr/pbx4*$^{-/-}$ nVII motor neurons (arrow) fail to migrate out of r4 in a wild-type host, while *lzr/pbx4*$^{-/-}$ nV motor neurons (arrowheads) always extend axons correctly from lateral r2 when placed in a wild-type embryo. (D) In the reciprocal experiment, wild-type nVII motor neurons in a *lzr/pbx4*$^{-/-}$ host migrate out of r4 and into more posterior rhombomeres (arrows), while wild-type nV axons (small arrowheads) often misroute from r4 with the nVII nerve. (E) Presumptive nVII motor neurons from a *hoxb1aMO*-injected donor fail to migrate in a wild-type host. (F) Wild-type nVII motor neurons migrate posteriorly in a *hoxb1aMO*-injected host. Scale bar, 100 μm.

motor neurons themselves migrate. This analysis does not eliminate the possibility that facial motor neuron migration may also be promoted by interactions with non-motor neurons in the hindbrain. Indeed, analysis of mouse-chick chimeras has elegantly demonstrated that signals from the caudal rhombomeres induce posterior migration of facial motor neurons (Studer, 2001). Community effects that promote neuronal migration have been described during Purkinje cell migration (Yang et al., 1993) and in the tangential chain migrations of olfactory neurons from the subventricular zone to the olfactory bulb in mammals (Lois et al., 1996; Wichterle et al., 1997); however, their genetic basis is poorly understood. Genetic analysis of facial motor neuron migration in the zebrafish may help to identify the molecules that mediate interactions between migrating neurons in the vertebrate brain.

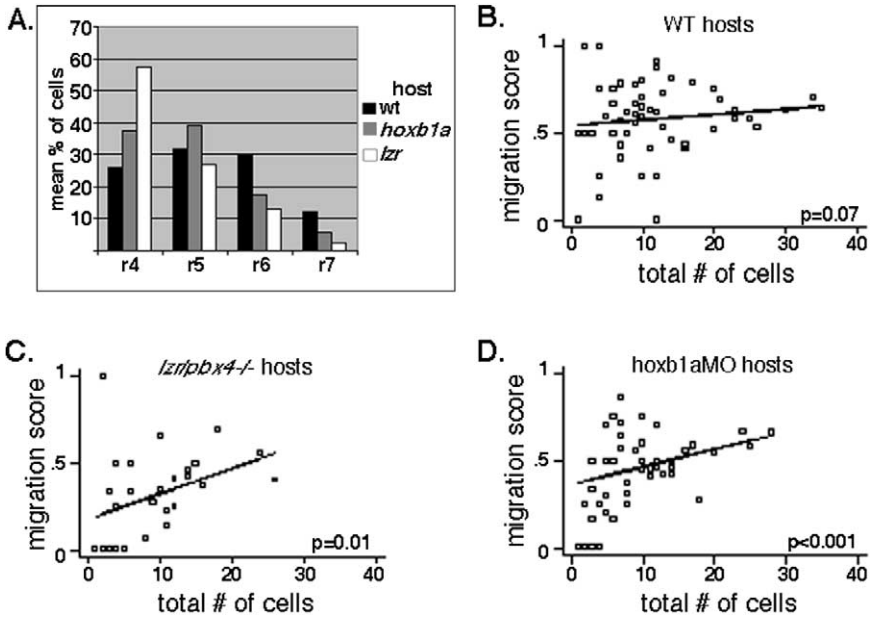

Fig. 6. Wild-type donor-derived facial motor neurons migrate farther in wild-type hosts than in either *lzr/pbx4*$^{-/-}$ or *hoxb1aMO* hosts, and the extent of migration in mutant hosts positively correlates with the number of donor-derived facial motor neurons. (A) Histogram plot illustrating the average percentage of wild-type donor motor neurons per embryo located in each of r4–r7 for wild-type, *lzr/pbx4*$^{-/-}$, and *hoxb1aMO* host genotypes. (B–D) Individual host embryos were also assigned a migration score based on the overall extent of facial motor neuron migration (see Materials and methods). The migration scores were plotted with respect to the number of wild-type donor facial motor neurons in each embryo (circles). Solid lines represent the fitted values based on a weighted linear regression analysis to correlate extent of migration with number of donor motor neurons per embryo. *P* values are shown for a test of the slope of the line = 0.

Lzr/pbx4 is required for Hoxa2 function and controls trigeminal axon pathfinding non-cell-autonomously

It is less clear how *lzr/pbx4* controls trigeminal motor axon pathfinding. The axon pathfinding defect in *lzr/pbx4* mutants resembles that of *Hoxa2* mutants in the mouse (Gavalas et al., 1997), and we show here that *lzr/pbx4* is required for *hoxa2* gain-of-function effects. *hoxa2* is expressed throughout r2 and r3, including in trigeminal motor neurons, as well as in the second pharyngeal arch (Prince et al., 1998). Hox PG2 proteins have a canonical Pbx-interacting "hexapeptide" motif; however, they have not been shown to bind Pbx proteins in vitro and no direct Hox PG2 targets have been identified. Furthermore, injection of *hoxa2* and *hoxb2* morpholinos, which reduce Hoxa2 and Hoxb2 protein levels in vitro by 72 and 65% respectively, fails to produce a comparable trigeminal motor axon phenotype in zebrafish (data not shown), although it is sufficient to cause duplication and fusion of first arch structures (Hunter and Prince, 2002). Given that the branchial arches are more sensitive to loss of *hoxa2* than is the neural tube in mice (Ohnemus et al., 2001), morpholino knock-down may not be sufficient to cause the neural tube defects that would lead to trigeminal axon defects in the fish. Thus, although our data are consistent with a role for *lzr/pbx4* as a *hoxa2* partner, we cannot unambiguously attribute the trigeminal pathfinding phenotype we observe in *lzr/pbx4* mutants specifically or exclusively to loss of *hoxa2* and/or *hoxb2* function.

We show here that *lzr/pbx4*$^{-/-}$ trigeminal motor axons always pathfind correctly in a wild-type host embryo, while wild-type trigeminal motor axons in a *lzr/pbx4*$^{-/-}$ host often misroute out of r4 with the facial nerve. The non-cell-autonomy of *lzr/pbx4* function indicates that *lzr/pbx4* does not function within motor neurons in r2 and r3 to specify their trigeminal motor identity. Rather, *lzr/pbx4*-dependent cue(s) from as-yet unidentified source(s) may cause trigeminal axons to pathfind correctly into the first arch. Possible sources of these signals include the branchial arches, which have been shown to have chemoattractive and growth-promoting properties for hindbrain motor axons (Caton et al., 2000). Furthermore, second arch-specific repulsive cues (Bell et al., 1999) may be lost in *lzr/pbx4* mutants along with second arch-specific *hox* gene expression (Pöpperl et al., 2000), allowing inappropriate pathfinding of trigeminal motor axons into the second arch. The central process of the trigeminal sensory nerve, which enters the hindbrain in r2, and the trigeminal sensory ganglia have also been shown to be required for trigeminal motor axon outgrowth (Moody and Heaton, 1983a,b; Caton et al., 2000); however, both of these are present in *lzr/pbx4*$^{-/-}$ embryos (Pöpperl et al., 2000; data not shown). Finally, short-range cues within the hindbrain that prevent trigeminal axons from projecting posteriorly may be affected in *lzr/pbx4*$^{-/-}$ embryos, where

patterning of r3 is abnormal (Pöpperl et al., 2000; Waskiewicz et al., 2002).

While our mosaic analysis shows that *lzr/pbx4* function is not required within the trigeminal motor neurons for their fate specification, a secondary *lzr/pbx4*-dependent non-autonomous cue from within the rhombomeres could influence motor neuron identity in r2 and r3. Indeed, Pbx function is required to establish an Fgf signaling center in r4 that specifies the identities of adjacent rhombomeres (Waskiewicz et al., 2002; Maves et al., 2002; Walshe et al., 2002). It is possible that Fgfs or other rhombomere-restricted signals influence motor neuron identity and therefore pathfinding in r2 and r3. We note that the possible sources of *lzr/pbx4*-dependent signals that influence trigeminal specification and/or pathfinding are not mutually exclusive, and the misrouting of trigeminal axons from r4 results in loss-of-function of *lzr/pbx4* in more than one location. Localized activation of wild-type *lzr/pbx4* activity in *lzr/pbx4*$^{-/-}$ embryos by RNA uncaging (Ando et al., 2001) combined with genetic mosaic analysis will help to define where *lzr/pbx4* is required for proper axon pathfinding.

Acknowledgments

We would like to thank Paul Grant for initial investigations into interaction amongst migrating facial motor neurons. Shin-ichi Higashijima and Hitoshi Okamoto generously provided the Is11-GFP transgenic line. We wish to thank Michèle Studer, Anand Chandrasekhar, Vicky Prince, and Dave Raible for their helpful comments on the manuscript. K.L.C is supported by a NSF Graduate Research Fellowship. C.B.M. is an assistant investigator of the Howard Hughes Medical Institute. This work was supported by NIH Grant #HD37909-01 and NSF Grant #IBN-9816905 (to C.B.M).

References

Amores, A., Force, A., Yan, Y.L., Joly, L., Amemiya, C., Fritz, A., Ho, R.K., Langeland, J., Prince, V., Wang, Y.L., Westerfield, M., Ekker, M., Postlethwait, J.H., 1998. Zebrafish *hox* clusters and vertebrate genome evolution. Science 282, 1711–1714.

Ando, H., Furuta, T., Tsien, R.Y., Okamoto, H., 2001. Photo-mediated gene activation using caged RNA/DNA in zebrafish embryos. Nat. Genet. 28, 317–325.

Auclair, F., Valdez, N., Marchand, R., 1996. Rhombomere-specific origin of branchial and visceral motoneurons of the facial nerve in the rat embryo. J. Comp. Neurol. 369, 451–461.

Bell, E., Wingate, R.J., Lumsden, A., 1999. Homeotic transformation of rhombomere identity after localized *Hoxb1* misexpression. Science 284, 2168–2171.

Bingham, S., Higashijima, S., Okamoto, H., Chandrasekhar, A., 2002. The zebrafish trilobite gene is essential for tangential migration of branchiomotor neurons. Dev. Biol. 242, 149–160.

Caton, A., Hacker, A., Naeem, A., Livet, J., Maina, F., Bladt, F., Klein, R., Birchmeier, C., Guthrie, S., 2000. The branchial arches and HGF are growth-promoting and chemoattractant for cranial motor axons. Development 127, 1751–1760.

Chandrasekhar, A., Moens, C.B., Warren Jr., J.T., Kimmel, C.B., Kuwada, J.Y., 1997. Development of branchiomotor neurons in zebrafish. Development 124, 2633–2644.

Garel, S., Garcia-Dominguez, M., Charnay, P., 2000. Control of the migratory pathway of facial branchiomotor neurones. Development 127, 5297–5307.

Gavalas, A., Davenne, M., Lumsden, A., Chambon, P., Rijli, F.M., 1997. Role of *Hoxa- 2* in axon pathfinding and rostral hindbrain patterning. Development 124, 3693–3702.

Gilland, E., Baker, R., 1993. Conservation of neuroepithelial and mesodermal segments in the embryonic vertebrate head. Acta Anat. (Basel) 148, 110–123.

Goddard, J.M., Rossel, M., Manley, N.R., Capecchi, M.R., 1996. Mice with targeted disruption of *Hoxb-1* fail to form the motor nucleus of the VIIth nerve. Development 122, 3217–3228.

Gurdon, J.B., Lemaire, P.L., Kato, K., 1993. Community effects and related phenomena in development. Cell 75, 831–834.

Hanneman, E., Trevarrow, B., Metcalfe, W.K., Kimmel, C.B., Westerfield, M., 1988. Segmental pattern of development of the hindbrain and spinal cord of the zebrafish embryo. Development 103, 49–58.

Higashijima, S., Hotta, Y., Okamoto, H., 2000. Visualization of cranial motor neurons in live transgenic zebrafish expressing green fluorescent protein under the control of the *1slet-1* promoter/enhancer. J. Neurosci. 20, 206–218.

Hunt, P., Gulisano, N., Cook, M., Sham, M.-H., Faiella, A., Wilkinson, D., Boncinelli, E., Krumlauf, R., 1991. A distinct *Hox* code for the branchial region of the vertebral head. Nature 353, 861–864.

Hunter, M.P and Price V.P., 2002. Zebrafish Hox paralogue group 2 genes function redundantly as selector genes to pattern the second pharyngeal arch. Dev. Biol. 247, 367–389.

Jacob, J., Guthrie, S., 2000. Facial visceral motor neurons display specific rhombomere origin and axon pathfinding behavior in the chick. J. Neurosci. 20, 7664–7671.

Jessen, J.R., Topczewski, J., Bingham, S., Sepich, D.S., Marlow, F., Chandrasekhar, A., Solnica-Krezel, L., 2002. Zebrafish trilobite identifies new roles for Strabismus in gastrulation and neuronal movements. Nat. Cell Biol. 4, 610–615.

Jungbluth, S., Bell, E., Lumsden, A., 1999. Specification of distinct motor neuron identities by the singular activities of individual Hox genes. Development 126, 2751–2758.

Keynes, R., Lumsden, A., 1990. Segmentation and the origin of regional diversity in the vertebrate central nervous system. Neuron 4, 1–9.

Kimmel, C.B., Ballard, W.W., Kimmel, S.R., Ullmann, B., Schilling, T.F., 1995. Stages of embryonic zebrafish. Dev. Dyn. 203, 253–310.

Lois, C., Garcia-Verdugo, J.M., Alvarez-Buylla, A., 1996. Chain migration of neuronal precursors. Science 271, 978–981.

Lumsden, A., Keynes, R., 1989. Segmental patterns of neuronal development in the chick hindbrain. Nature 337, 424–428.

Mann, R., Chann, S-K., 1996. Extra specificity from *extradenticle*: the partnership between HOX and PBX/EXD homeodomain proteins. Trends Genet. 12, 772–774.

Maves, L., Jackman, W., Kimmel, C., 2002. FGF3 and FGF8 mediate a rhombomere 4 signaling activity in the zebrafish hindbrain. Development 129, 3825–3837.

McClintock, J.M., Carlson, R., Mann, D.M., Prince, V.E., 2001. Consequences of *Hox* gene duplication in the vertebrates: an investigation of the zebrafish *Hox* paralogue group 1 genes. Development 128, 2471–2484.

McClintock, J.M., Kheirbek, M.A., Prince, V.E., 2002. Knockdown of duplicated zebrafish hoxb1 genes reveals distinct roles in hindbrain patterning and a novel mechanism of duplicate gene retention. Development 129, 2339–2354.

Moens, C.B., Fritz, A., 1999. Techniques in neural development. Methods Cell Biol. 59, 253–272.

Moody, S.A., Heaton, M.B., 1983a. Developmental relationships between trigeminal ganglia and trigeminal motoneruons in chick embryos. II. Ganglion axon ingrowth guides motoneuron migration. J. Comp. Neurol. 213, 344–349.

Moody, S.A., Heaton, M.B., 1983b. Developmental relationships between trigeminal ganglia and trigeminal motorneurons in chick embryos. I. Ganglion development is necessary for motorneuron development. J. Comp. Neurol. 213, 327–343.

Nasevicius, A., Ekker, S.C., 2000. Effective targeted gene "knockdown" in zebrafish. Nat. Genet. 26, 216–220.

Ohnemus, S., Bobola, N., Kanzler, B., Mallo, M., 2001. Different levels of Hoxa2 are required for particular developmental processes. Mech. Dev. 108, 135–147.

Pöpperl, H., Bienz, M., Studer, M., Chan, S.K., Aparicio, S., Brenner, S., Mann, R.S., Krumlauf, R., 1995. Segmental expression of *Hoxb-1* is controlled by a highly conserved autoregulatory loop dependent upon *exd/pbx*. Cell. 81, 1031–1042.

Pöpperl, H., Rikhof, H., Cheng, H., Haffter, P., Kimmel, C.B., Moens, C.B., 2000. *lazarus* is a novel *pbx* gene that globally mediates *hox* gene function in zebrafish. Mol. Cell 6, 255–267.

Prince, V.E., Moens, C.B., Kimmel, C.B., Ho, R.K., 1998. Zebrafish *hox* genes: expression in the hindbrain region of wild-type and mutants of the segmentation gene, *valentino*. Development 125, 393–406.

Studer, M., Lumsden, A., Ariza-McNaughton, L., Bradley, A., Krumlauf, R., 1996. Altered segmental identity and abnormal migration of motor neurons in mice lacking *Hoxb-1*. Nature 384, 630–634.

Studer, M., Gavalas, A., Marshall, H., Ariza-McNaughton, L., Rijli, F.M., Chambon, P., Krumlauf, R., 1998. Genetic interactions between *Hoxa1* and *Hoxb1* reveal new roles in regulation of early hindbrain patterning. Development 125, 1025–1036.

Studer, M., 2001. Initiation of facial motoneurone migration is dependent on rhombomeres 5 and 6. Development 128, 3707–3716.

Trevarrow, B., Marks, D.L., Kimmel, C.B., 1990. Organization of hindbrain segments in the zebrafish embryo. Neuron 4, 669–679.

Turner, D.L., Weintraub, H., 1994. Expression of *achaete-scute* homolog 3 in Xenopus embryos converts ectodermal cells to a neural fate. Genes Dev. 8, 1434–1447.

Vlachakis, N., Ellstrom, D.R., Sagerstrom, C.G., 2000. A novel *pbx* family member expressed during early zebrafish embryogenesis forms trimeric complexes with Meis3 and Hoxb1b. Dev. Dyn. 217, 109–119.

Vlachakis, N., Choe, S., Sägerstrom, C.G., 2001. *Meis3* synergizes with *Pbx4* and *Hoxb1b* in promoting hindbrain fates in the zebrafish. Development 128, 1299–1312.

Walshe, J., Maroon, H., McGonnell, I.M., Dickson, C., Mason, I., 2002. Establishment of hindbrain segmental identity requires signalling by FGF3 and FGF8. Curr. Biol. 12, 1117–1123.

Waskiewicz, A.J., Rikhof, H.A., and Moens, C.B. (2002). Eliminating zebrafish pbx proteins reveals a hindbrain ground state. Dev. Cell 3, 723–733.

Westerfield, M., 1995. The Zebrafish Book: A Guide for the Laboratory Use of Zebrafish (*Danio rerio*). University of Oregon Press, Eugene, OR.

White, H., 1980. A heteroskedasticity-consistent covariance matrix estimator and a direct test for heteroskedasticity. Econometrica 48, 817–830.

Wichterle, H., Garcia-Verdugo, J.M., Alvarez-Buylla, A., 1997. Direct evidence for homotypic, glia-independent neuronal migration. Neuron 18, 779–791.

Wilkinson, D.G., Bhatt, S., Cook, M., Boncinelli, E., Krumlauf, R., 1989. Segmental expression of *Hox-2* homeobox-containing genes in the developing mouse hindbrain. Nature 341, 405–409.

Woo, K., Fraser, S.E., 1995. Order and coherence in the fate map of the zebrafish nervous system. Development 121, 2595–2609.

Yan, Y.L., Jowett, T., Postlethwait, J.H., 1998. Ectopic expression of *hoxb2* after retinoic acid treatment or mRNA injection: disruption of hindbrain and craniofacial morphogenesis in zebrafish embryos. Dev. Dyn. 213, 370–385.

Yang, H., Jensen, P., Goldowitz, D., 1993. The community effect and Purkinje cell migration in the cerebellar cortex: analysis of *scrambler* chimeric mice. J. Neurosci. 22, 464–470.